Journal of Applied Sciences

ISSN 1812-5654

science alert

ANSInet
an open access publisher
http://ansinet.com

Journal of Applied Sciences 14 (24): 3455-3463, 2014
ISSN 1812-5654 / DOI: 10.3923/jas.2014.3455.3463

Adsorption of Phosphorus Using Water Treatment Sludge

Beverly S. Chittoo and Clint Sutherland
Department of Project Management and Civil Infrastructure Systems,
University of Trinidad and Tobago, Trinidad

Abstract: In line with global sustainable development the search for cost effective and eco-friendly disposal options for water treatment sludge continues to be an urgent priority. In this study, the phosphate adsorption potential of three types of water treatment sludge, namely; alum sludge, lime sludge and lime-iron sludge were investigated through a series of batch experiments. All three sludges exhibited potential for phosphate removal however; lime-iron sludge produced the highest adsorption capacity which was 34 and 52% higher than that for lime sludge and alum sludge, respectively. Phosphate adsorption using alum sludge favoured slightly acidic conditions (pH 4) while lime sludge and lime-iron sludge favoured slightly basic conditions at pH 8. Mathematical simulation of the adsorption process was conducted using linear and non-linear regression. Adsorption kinetics was analyzed using the pseudo-first-order, pseudo-second-order, intraparticle diffusion and diffusion-chemisorption models. The goodness of fit was assessed using the coefficient of determination (R^2), the Relative Percent Error (RPE) Marquardt's Percent Standard Deviation (MPSD) and Hybrid Error Function (HYBRID). The diffusion-chemisorption model produced the highest correlation to reaction variables for all sludges tested. It was successfully used to predict process kinetics which can aid in the eventual development of full-scale design.

Key words: Adsorption, water treatment sludge, lime-iron sludge, lime sludge, alum sludge phosphate, kinetics

INTRODUCTION

Domestic wastewater usually contain phosphorus, an essential constituent of living matter and a crucial element for agricultural and numerous industrial activities. However, the presence of phosphorus in effluent, above permissible discharge levels, often leads to eutrophication in lakes and streams and the subsequent deterioration in water quality; which may significantly increase the cost of water treatment. Parallel to this, global reserves of phosphorus (a non-renewable resource) are estimated to be depleted or near totally deleted by 2050 (Farrell, 2012). As such, more efforts have been made in recent years, towards recovering phosphorus from wastewater.

Physical-chemical processes such as ion exchange, dissolved air flotation, membrane filtration, high rate sedimentation, coagulation and adsorption are used extensively for phosphorus removal from wastewater. According to Mohammed and Rashid (2012), adsorption is one of the most common techniques in current use. However, the acquisition of adsorbents which are both easily available and efficient, remains a significant challenge in small-scale wastewater applications.

According to Razali *et al*. (2007), water treatment sludge exhibits significant potential for phosphorus reduction during wastewater treatment. They highlighted that aluminum or iron hydroxides are the important adsorption components of water treatment sludge once it has been dewatered. These key components have also been identified by Kim *et al*. (2003). Additionally, Kim *et al*. (2003) and Ippolito *et al*. (2003) indicated that the presence of calcium in water treatment sludge may influence phosphorus removal via precipitation.

Although adsorption of phosphorus by water treatment sludge has been well documented, studies have focused predominantly on the use of alum sludge as an adsorbent with little information on the effectiveness of other types of water treatment sludge. Mortula and Gagnon (2007) found that dried alum residuals were a better media for phosphorus adsorption than other waste materials, including blast furnace slag, cement kiln dust and bone char. Tie *et al*. (2010) reported a 98% phosphate adsorption capacity by alum sludge and a 95% adsorption capacity by lime sludge. Ippolito *et al*. (2003) showed that alum based water treatment residuals had a high phosphorus-binding capacity of approximately 12.5 g P/kg water treatment sludge while Dayton and Basta (2001) reported phosphorus-binding capacities ranging from 10.4-37.0 g P/kg water treatment sludge by examining 18 types of sludges in the United States of America.

Corresponding Author: Clint Sutherland, Department of Project Management and Civil Infrastructure Systems, University of Trinidad and Tobago, Trinidad Tel: 868 497 5744 Fax: 868 223 1621

For this study, the adsorption of orthophosphate by three types of water treatment sludge (alum sludge, lime sludge and lime-iron sludge) was investigated using batch experiments with phosphate concentrations typical of municipal wastewater. Experimental data was fitted to four commonly used kinetic models: Lagergren pseudo-first-order model (Lagergren, 1898); pseudo-second-order model (Ho and McKay, 1998b); Weber and Morris intraparticle model (Weber and Morris, 1962) and the diffusion-chemisorption model (Sutherland, 2004). The modelled data was analyzed in an attempt to explicate the adsorption parameters and to select an appropriate kinetic model to aid in the eventual development of predictive models for full scale design of adsorption systems.

MATERIALS AND METHODS

Adsorbent: Batch adsorption experiments were conducted using alum sludge, lime sludge and lime-iron sludge. Alum sludge, the residual generated when aluminum salt such as aluminum sulphate is used as a coagulant, was collected from the sludge landfill site at a water treatment plant located in west-central Trinidad. Lime sludge, produced when hydrated lime is used for water softening processes, was collected from the sludge pond at a water treatment plant located in south Trinidad. Lime-iron sludge, produced when hydrated lime is used for the precipitation of iron from water, was collected from the sludge pond at a water treatment plant located in central Trinidad. After collection, the water treatment sludge used in this study was heated in an oven at 105°C for 24 h. The oven dried sludge was then cooled to room temperature for 72 h which attain equilibrium moisture content of 12%. Sludge particles were subsequently pulverized using a mortar and pestle and sieved. Specimen passing a 2.36 mm sieve and retained on pan was collected for experimentation.

Preparation of synthetic waste water: Phosphate stock solution (10.5 mg L^{-1}) was prepared by dissolving 15 mg L^{-1} of orthophosphate salt (Potassium dihydrogen phosphate: Riedel De Haen KH_2PO_4, AnalaR grade) in distilled water.

Characterization of the water treatment sludge: Chemical analysis of the dewatered sludge was carried out using Energy Dispersive Spectroscopy and Atomic Adsorption Spectrophotometry. The morphological structure of the dewatered sludge was examined using a Scanning Electron Microscope (JEOL Scanning Electron Microscope JSM 6490 LV).

Batch kinetic tests: Kinetic studies for phosphate adsorption were conducted in triplicate in batch mode with an adsorbent mass of 0.5 g and spiked with 100 mL of synthetic phosphate solution (10.5 mg L^{-1}) in 250 mL Erlenmeyer flasks. Adsorbent masses were accurate to ±0.0001 g and solution volumes to ±0.5 mL. All experiments were carried out at 25°C±1. The effect of solution pH was studied within the range of 2-10. The pH of the phosphate solution was adjusted by adding 0.1 M sulphuric acid or 0.01 M sodium hydroxide and measured using a Multi-Parameter Meter (HACH HQ430d).

The reaction mixtures were agitated on a SK-330-Pro Orbital Shaker and stopped at predetermined time intervals (1, 2, 4, 8, 16, 20 and 24 h). The adsorbent was then separated by vacuum filtration using a Buchner's funnel and Whatman No. 3 qualitative filter paper. The filtrate was subsequently measured at a wavelength of 880 nm using an ultraviolet spectrophotometer (Shimadzu Recording Spectrophotometer UV-1800). A blank comprising distilled water and sludge was prepared to measure any background phosphate.

The amount of phosphate adsorbed per unit mass of adsorbent was obtained using the equation:

$$q_t = \frac{(C_O - C_e)V}{m} \quad (1)$$

where, q_t (mg g^{-1}) is mass of the adsorbate adsorbed per mass of adsorbent, C_0 (mg L^{-1}) is initial concentration of phosphate in solution, C_e (mg L^{-1}) is final concentration of phosphate in solution, V (l) is volume of synthetic phosphate solution, m (g) is mass of adsorbent.

Kinetic modelling of adsorption: According to Sutherland and Venkobachar (2010), the transport of an adsorbate from a liquid phase to an adsorbent's surface usually involves: (1) Transport from the bulk solution to the hydrodynamic film surrounding adsorbent particles, (2) Diffusion/mass transport through the hydrodynamic film by molecular diffusion which is influenced by the concentration difference and (3) Transfer of the adsorbate particles from the surface of the adsorbent to active sites within the adsorbent or on the external surface which is dependent on the size and pore structure of the adsorbent particle. Following the transportation phase, attachment to the adsorbent surface may occur via physical adsorption due to non-specific forces of attraction, electrostatic adsorption due to columbic forces of attraction or specific adsorption due to chemical forces of attraction.

For this study, experimental data was fitted to four commonly used kinetic models each of which was

developed on a different premise. The modelled data was analyzed in attempt to select the most appropriate kinetic equation to aid in the prediction of process kinetics and whose premise could elucidate the probable mechanism of phosphate adsorption onto water treatment sludge.

Kinetic models

Pseudo-first-order model: Lagergren (1898) presented a first-order rate equation to describe the kinetic process of liquid-solid phase adsorption of oxalic acid and malonic acid onto charcoal. The model assumes a first-order rate based on surface reactions. To distinguish kinetic equations based on adsorption capacity from solution concentration, Lagergren's first order rate equation has been called pseudo-first-order (Ho and McKay, 1998a). Non-linear and linear forms of the pseudo-first-order model are represented by Eq. 2 and 3, respectively in Table 1 where:

K_{PFO} = Rate constant of pseudo-first order adsorption (min^{-1})
q_t = The mg of phosphate absorbed/g of adsorbent at any time t (mg g^{-1})
q_e = Amount of adsorption at equilibrium (mg g^{-1})

The expressions have been successfully applied to adsorbents such as fly ash (Panday *et al*., 1985), China clay (Sharma *et al*., 1991) and Fe (III)/Cr (III) hydroxide (Namasivayam and Ranganathan, 1993).

Pseudo-second-order model: The pseudo-second-order equation by Ho and McKay (1998b), was developed for the adsorption of divalent metal ions onto peat moss. The model was developed on the premise that chemisorption is the operative reaction mechanism. Non-linear and linear forms of the pseudo-second-order model are represented by Eq. 4 and 5, respectively in Table 1 where:

K_{PSO} = Pseudo-second-order rate, (g mg^{-1} min^{-1})
q_t = The mg of phosphate adsorbed/g of adsorbent at any time (mg g^{-1})
q_e = Amount of adsorption at equilibrium (mg g^{-1})
h = Initial adsorption rate (mg g^{-1}-t)

The model has been successfully applied to several adsorbents including activated carbon (Sharma and Forster, 1996), algae (Fernadez *et al*., 1995) and peat (Ho *et al*., 1996).

Intraparticle diffusion model: The intraparticle diffusion model was developed by Weber and Morris (1962). The model is based on the assumption that intraparticle diffusion is the controlling mechanism of adsorption. Linear and non-linear forms of the model are given by Eq. 6 and 7, respectively in Table 1 where:

q_t = Adsorbate uptake at time t (mg g^{-1})
K_{id} = Rate constant of intraparticle transport (mg g^{-1}-$t^{1/2}$)

This model was shown by Krim *et al*. (2006) to be significant in modelling fungi adsorption of chromium at low concentrations. Rahman *et al*. (2013) showed that intraparticle diffusion is significant in modelling the adsorption of Remazol G Yellow RGB (an anionic reactive dye) onto acid activated vegetable kitchen waste at high concentrations.

Diffusion-chemisorption model: An empirical diffusion-chemisorption kinetic model was developed by Sutherland (2004) to simulate biosorption of heavy metals unto heterogeneous media. It is based on the assumption that both diffusion and chemisorption control the adsorption process. Linear and non-linear forms of the diffusion-chemisorption model are given by Eq. 8 and 9, respectively in Table 1 where:

Table 1: Linear and non-linear kinetic models

Model	Linear equation	Equation number	Non-linear equation	Equation number
Pseudo-first-order model	$\log(q_e - q_t) = \log q_e - \frac{K_{PFO}}{2.303}t$	2	$q_t = q_e(1 - \exp^{-K_1 t})$	3
Pseudo-second-order model	$\frac{t}{q_t} = \frac{1}{K_{PSO} q_e^2} + \frac{t}{q_e}$ $h = (K_{PSO})\, q_e^2$	4	$q_t = \frac{K_2 q_e^2 t}{1 + K_2 q_e t}$	5
Intraparticle diffusion model	$q_t = K_{id}(t^{1/2}) + c$	6	$q_t = K_{id}(t^{1/2})$	7
Diffusion-chemisorption model	$\frac{t^{0.5}}{q_t} = \frac{1}{q_e} \times t^{0.5} + \frac{1}{K_{DC}}$ $k_i = K_{DC}^2/q_e$	8	$q_t = \frac{1}{\frac{1}{q_e} + \frac{1}{K_{DC} \times t^{0.5}}}$	9

Table 2: Error functions

Error functions	Expression	Equation number
Relative Percent Error (RPE)	$\text{RPE (\%)} = \frac{\left[\frac{\left\lvert (q_e)_{predicted} - (q_e)_{experimental} \right\rvert}{(q_e)_{experimental}}\right] \times 100}{N}$ where, N is the number of experimental points	10
Marquardt's Percent Standard Deviation (MPSD)	$\text{MPSD} = 100\sqrt{\frac{1}{N-P}\sum_{i=1}^{N}\left[\frac{\left\lvert (q_e)_{experimental} - (q_{e_i})_{predicted} \right\rvert}{(q_{e_i})_{experimental}}\right]^2}$ where, N is the number of experimental points and P is the number of parameters in the regression model	11
Hybrid Error Function (HYBRID)	$\text{HYBRID} = \frac{100}{N-P}\sum_{i=1}^{N}\left[\frac{\left((q_e)_{experimental} - (q_{e_i})_{predicted}\right)^2}{(q_{e_i})_{experimental}}\right]$ where, N is the number of experimental points and P is the number of parameters in the regression model	12

K_{DC} = Diffusion-chemisorption constant (g mg^{-1} min^{-1})
q_t = The mg of phosphate adsorbed/g of sorbent at any time (mg g^{-1})
q_e = Amount of adsorption at equilibrium (mg g^{-1})
k_i = Initial adsorption rate (mg g^{-1}-t)

The diffusion-chemisorption model has been successfully used to simulated the adsorption process for adsorbents including a forest macro-fungus, *Fomes faciatus* (Sutherland and Venkobachar, 2010), *A. coriaria*, *Musa* spp., *E. abyssinica* (Bakyayita, 2014) and HCF-modified pine (Ofomaja *et al*., 2014).

Statistical analysis: The goodness of fit of the various kinetic models to the experimental data was evaluated by the coefficient of determination (R^2) the Relative Percent Error (RPE), the Marquardt's Percent Standard Deviation (MPSD) and the Hybrid Error Function (HYBRID) (Table 2).

RESULTS AND DISCUSSION

Composition of water treatment sludge: The principal elemental compositions of the dewatered sludges used in this study are shown in Table 3. Although the properties of such sludges are highly variable and dependent on the type of raw water and the type of treatment, it is clear that aluminum, calcium and iron were the dominant components of alum sludge, lime sludge and lime-iron sludge, respectively. These dominant components were also identified by Kim *et al*. (2003) as key components which aid in phosphorus removal via adsorption and precipitation.

Table 3: Composition of oven-dried water treatment sludge

Elements	Alum sludge	Lime sludge	Lime-iron sludge
	(weight %)		
Magnesium	0.16	1.20	0.61
Silicon	3.28	1.11	3.59
Chlorine	0.03	0.17	0.12
Calcium	0.12	32.72	27.26
Manganese	0.03	0.03	0.68
Iron	1.15	0.44	31.11
Cobalt	0.02	0.02	0.18
Zinc	-	0.60	0.14
Sodium	0.26	0.24	-
Aluminum	31.52	3.76	-
Potassium	0.41	0.07	-
Titanium	0.10	0.05	-
Mercury	0.31	-	-

Morphological structure of water treatment sludge: The water treatment sludge used in the study was oven dried within 48 h of collection. According to Hayden and Rubin (1976), aging increases the crystallinity of the precipitate. Crystallinity reduces the specific surface area of the precipitate which is directly related to the number of hydroxide sites available for adsorption (Duffy and van Loon, 1994). Gibbons *et al*. (2009) further iterated that drying within 30 days of collection minimizes the change from amorphous to crystalline form and thus ensures that the residuals have a maximum number of hydroxide sites available for adsorption. Scanning Electron Microscope (SEM) images of the powdered sludge, illustrated in Fig. 1a-c, were used to further verify its amorphous structure. The SEM images were similar to those obtained by Yang *et al*. (2006a, b).

Kinetic analysis using linear regression: Linear regression was performed by applying the linearized form of the kinetic equations to the experimental data. The

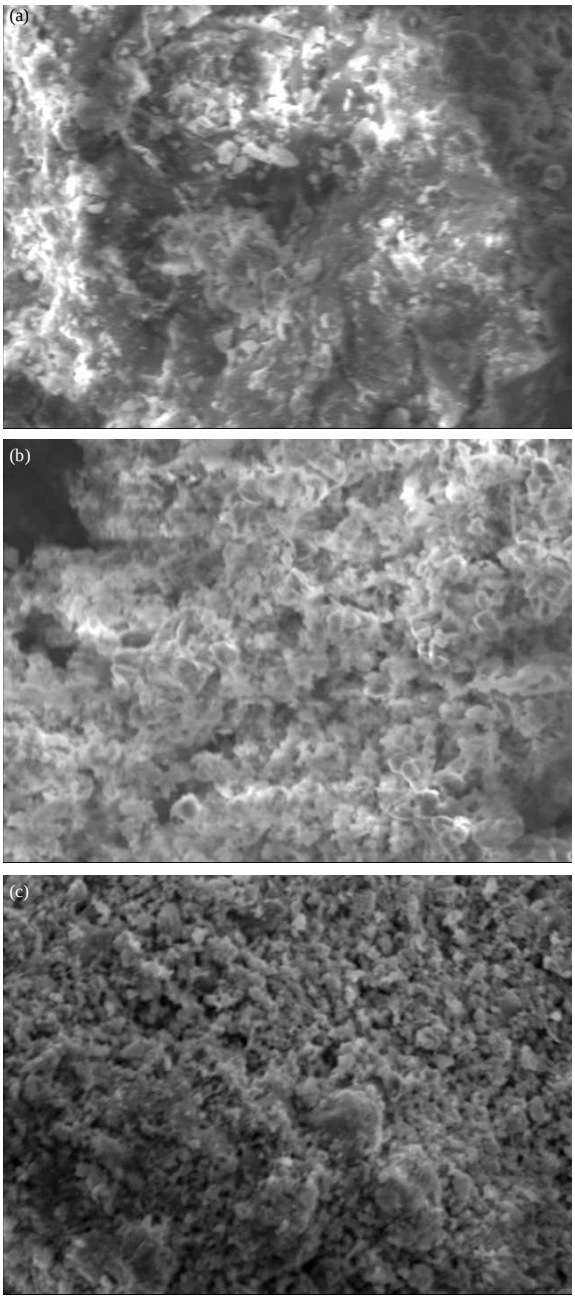

Fig. 1(a-c): SEM observation of powdered (a) Alum sludge (1000X), (b) Lime sludge (1000X) and (c) Lime-iron sludge (1000X)

coefficients of determination (R^2), obtained from linearization for alum sludge, lime sludge and lime-iron sludge are presented in Table 4, respectively.

Linearized plots using the pseudo-first-order model for both alum sludge and lime sludge revealed correlation coefficients (R^2); consistently greater than 0.86 while lime-iron sludge showed lower conformity. A comparison of the non-linear experimental curves to theoretical curves (generated using values of q_e and K_{PFO} obtained from linearization) was performed by calculating the RPE, MPSD and HYBRID error functions (Table 2). The error values (Table 4) also confirmed the poor simulation by the model. The experimental data was subsequently modelled using the intraparticle diffusion equation. The curves did not pass through the origin. Badmus *et al*. (2007) indicated that such deviation from the origin implies that intraparticle transport is not the rate limiting step. In all instances an increase in intercept was observed with increase in agitation. This does not discount the presence of intraparticle diffusion, however, it does signal the possible existance of film diffusion.

The correlation coefficients for the linearized pseudo-second-order plots were generally closer to unity (>0.998) for the three sludges. The equation parameters obtained from linearized plots were subsequently used to generate theoretical kinetic curves and were compared to the primary kinetic curves by calculating the RPE, MPSD and HYBRID error values. These values which are also presented in Table 4 showed good conformity to the model. This implies that chemisorption involving valency forces through sharing or exchange of electrons between adsorbent and adsorbate may be the dominant mechanism of adsorption (Ho and McKay, 1998b).

The linearized diffusion-chemisorption plots also showed good correlation for all three sludges with correlation coefficients consistently greater than 0.997. RPE, MPSD and HYBRID error values obtained by comparing the primary kinetic curves and the theoretical curves generated using linearized parameters (Table 4) showed good conformity to the model. This suggests that adsorption may be a multi-mechanistic reaction in which, beyond the initial film diffusion controlled region, the process is controlled by intraparticle diffusion followed by chemisorption (Sutherland and Venkobachar, 2010).

Although both linearized pseudo-second-order and diffusion-chemisorption models provide a suitable level of precision to the data, it is prudent to further assess simulations using non-linear regression. According to Kumar and Sivanesan (2006) the different axial setting of each linearized model may alter the error distribution and the kinetic parameters. In order to minimize the impact of linearization on predicting the best fit kinetic expression, non-linear regression which is often considered a more robust method of optimization is used. This is particularly valuable when attempting to predict process performance.

Table 4: Comparison of kinetic models using error functions and linear and non-linear regression to simulate alum, lime and lime-iron sludge uptake of phosphate

			Linear regression			Non-linear regression		
Agitation	Model	Linearized (R^2)	RPE	MPSD	HYBRID	RPE	MPSD	HYBRID
Alum slugle uptak of phosphate								
150 rpm	Pseudo-first-order	0.9797	80.24	99.03	112.36	9.27	13.22	2.22
	Pseudo-second-order	0.9987	5.66	9.11	0.82	2.62	4.45	0.23
	Intraparticle diffusion	0.9272	75.25	92.98	98.86	30.76	46.37	22.03
	Diffusion-chemisorption	0.9971	2.12	3.53	0.14	2.23	3.44	0.13
250 rpm	Pseudo-first-order	0.8623	84.10	103.51	128.62	5.08	6.92	0.57
	Pseudo-second-order	0.9982	4.84	8.75	0.82	3.10	3.83	0.18
	Intraparticle diffusion	0.9476	82.12	101.02	122.65	33.07	48.83	26.37
	Diffusion-chemisorption	0.9968	7.58	10.04	1.25	1.75	2.42	0.07
350 rpm	Pseudo-first-order	0.967	53.00	66.27	53.27	3.35	4.51	0.25
	Pseudo-second-order	0.9993	1.65	2.32	0.07	1.65	2.24	0.06
	Intraparticle diffusion	0.8371	85.36	104.86	136.30	33.75	50.26	29.10
	Diffusion-chemisorption	0.9981	1.73	2.14	0.06	1.49	2.09	0.06
Lime sludge uptake of phosphate								
150 rpm	Pseudo-first-order	0.9568	83.72	102.880	131.50	1.38	2.19	0.06
	Pseudo-second-order	1.0000	1.86	3.7000	0.15	1.90	3.41	0.13
	Intraparticle diffusion	0.7034	80.27	98.860	121.07	33.05	48.64	26.75
	Diffusion-chemisorption	0.9969	3.34	6.090	0.38	3.41	5.68	0.35
250 rpm	Pseudo-first-order	0.9169	86.18	105.880	141.60	3.80	5.15	0.34
	Pseudo-second-order	0.9995	4.04	7.150	0.59	2.02	2.93	0.11
	Intraparticle diffusion	0.9655	86.38	106.060	142.25	33.83	50.18	29.90
	Diffusion-chemisorption	0.9990	1.60	2.200	0.06	1.27	1.84	0.04
350 rpm	Pseudo-first-order	0.9562	91.86	112.630	164.47	2.77	4.34	0.24
	Pseudo-second-order	0.9999	1.50	3.2500	0.13	1.17	1.91	0.04
	Intraparticle diffusion	0.9039	89.55	109.840	156.31	35.06	51.40	32.49
	Diffusion-chemisorption	0.9999	0.68	1.0100	0.01	0.66	1.00	0.01
Lime-iron sludge uptake of phosphate								
150 rpm	Pseudo-first-order	0.9709	83.79	103.04	194.34	3.09	4.11	0.31
	Pseudo-second-order	0.9999	1.54	2.55	0.10	7.45	9.73	1.86
	Intraparticle diffusion	0.8381	80.84	99.52	181.05	32.95	48.70	39.54
	Diffusion-chemisorption	0.9995	1.38	2.44	0.10	1.46	2.41	0.09
250 rpm	Pseudo-first-order	0.6709	92.83	113.78	247.38	2.43	2.39	0.11
	Pseudo-second-order	0.9999	0.77	1.32	0.03	9.00	11.13	2.41
	Intraparticle diffusion	0.7144	88.62	108.72	225.43	35.25	51.38	47.41
	Diffusion-chemisorption	0.9993	1.56	2.66	0.12	1.62	2.25	0.09
350 rpm	Pseudo-first-order	0.8938	92.16	113.01	221.74	2.49	3.43	0.21
	Pseudo-second-order	0.9993	3.29	5.47	0.48	1.28	1.88	0.06
	Intraparticle diffusion	0.8783	88.95	109.12	206.55	34.88	51.10	42.97
	Diffusion-chemisorption	0.9989	1.11	1.76	0.05	1.23	1.69	0.05

Kinetic analysis using non-linear regression: Non-linear regression analysis was performed using the non-linear form of the kinetic equations presented in Table 1. The results for alum sludge, lime sludge and lime-iron sludge are also presented in Table 4. With the exception of the intraparticle diffusion model, the other tested models showed good conformity to the experimental data. However, closer analysis of the RPE, MPSD and HYBRID error functions revealed that the diffusion-chemisorption model generally produced the highest correlation within the range of agitation tested for all three sludges. A comparison of the error values obtained from linear and non-linear regression indicated that non-linear regression was generally able to produce a more robust simulation over that of linear regression. Hence, the diffusion-chemisorption model was selected for further analysis of the adsorption processes.

Effect of agitation on adsorption: Nomanbhay and Palanisamy (2005) explained that with increased agitation, the diffusion rate of adsorbate from the solution to the liquid boundary layer surrounding the adsorbent particles increases due to the enhancement of turbulence and a decrease in the thickness of the liquid boundary layer. This consequently increases the rate of adsorption. A similar trend was observed in this investigation. The overall rate, K_{DC} as well as the initial rate of adsorption, k_i increased with increase in agitation for the three types of sludges (Table 5) and thus verifies to importance of diffusion in the reaction.

The change in both K_{DC} and, k_i as the agitation increased from 250-350 rpm was marginal compared to the changes observed as agitation increased from 150-250 rpm. This reduction may be attributed to an increase desorption tendency of adsorbate molecules

Table 5: Diffusion-chemisorption model parameters obtained by non-linear regression for water treatment sludge uptake of phosphate at varying rates of agitation

		Diffusion-chemisorption		
Adsorbent	Agitation (rpm)	K_{DC}	q_e (mg g^{-1})	k_i
Alum sludge	150	2.3577	1.5069	3.6889
	250	3.5680	1.4390	8.8469
	350	4.3239	1.4389	12.9933
Lime sludge	150	3.0180	1.5461	5.8912
	250	5.0931	1.4375	18.0450
	350	6.6148	1.4297	30.6047
Lime-iron sludge	150	4.7423	2.2505	9.9931
	250	8.1844	2.1448	31.2311
	350	8.4142	1.9250	36.7786

Table 6: Diffusion-chemisorption model parameters obtained by non-linear regression for water treatment sludge uptake of phosphate at varying pH

		Diffusion-chemisorption		
Sorbent	pH	K_{DC}	q_e (mg g^{-1})	k_i
Alum sludge	2	5.8967	0.8206	42.37
	4	7.5943	1.1249	51.27
	7	5.5232	1.0671	28.59
	9	0.8741	1.0843	0.70
Lime sludge	8	2.9065	1.5236	5.54
	9	2.6343	1.3275	5.23
	10	1.8608	1.3526	2.56
Lime-iron sludge	8	4.6610	2.3131	9.39
	9	2.2942	2.2348	2.36
	10	1.5915	2.2249	1.14

resulting from vigorous mixing which displaces adsorbate molecules from active sites. Furthermore, an increase in agitation from 250-350 rpm necessitates higher energy input which consequently increases operation cost. Hence, 250 rpm was selected as the optimum agitation for this experiment.

The overall rate of adsorption (K_{DC}) and the initial rate (k_i) were highest for lime-iron sludge followed by lime sludge and finally alum sludge thus indicating the significance of lime-iron sludge as an adsorbent for phosphate.

Effect of pH on adsorption: The effect of solution pH was investigated at a constant phosphate concentration (10.5 mg L^{-1}), adsorbent dose (0.5 g) and agitation (250 rpm). The results presented in Table 6 indicate that the three sludges were sensitive to pH. In the case of alum sludge, the overall adsorption rate (K_{DC}) and initial rate (k_i) was highest at pH 4 and fluctuated with change in pH. Additionally, the maximum adsorption capacity q_e of 1.125 mg g^{-1} was obtained at pH 4. This is consistent with the results reported by Kim *et al*. (2003) and Yang *et al*. (2006b) who indicated that phosphate adsorption by alum sludge favoured a slightly acidic condition. The trend in adsorption using lime-iron sludge was similar to that of lime sludge. The K_{DC} and k_i were greatest at pH 8 and decreased progressively as the pH increased. The maximum adsorption capacity, q_e for lime sludge and lime-iron sludge was 1.523 and 2.313 mg L^{-1}, respectively.

According to Liu *et al*. (2002) depending on the solution pH, phosphate species can exist as H_3PO_4, $H_2PO_4^-$, HPO_4^{2-} and PO_4^{3-}. The authors further stated that at pH = 3.0, the predominant specie of phosphate is H_3PO_4 which is weakly attached to adsorption sites. For solution pH within the range 4-10 the dominant species are $H_2PO_4^-$ and HPO_4^{2-} which can be readily adsorbed. However, as the pH increases beyond 10, PO_4^{3-} becomes the dominant specie and phosphorus adsorption reduces due to competition between PO_4^{3-} and OH^- for active sites on the sludge surface, electrostatic repulsion and the counter ion layer formed by OH^- ions adsorbed on the sludge.

For the three sludges tested, equilibrium was reached after 6 h of reaction. At optimum conditions, though alum sludge had the highest overall adsorption rate (K_{DC}) and initial rate (k_i), its adsorption capacity q_e was lowest amongst the sludges tested (Table 6). Lime-iron sludge produced the highest adsorption capacity which was 34 and 52% higher than that for lime sludge and alum sludge, respectively. Given the significantly higher adsorption capacity, lime-iron sludge appeared to be a better phosphate adsorbent than alum sludge and lime sludge. This is consistent with the results obtained by Genz *et al*. (2004) who indicated that iron-based adsorbents were more effective for phosphate adsorption than aluminum-based adsorbents.

Effect of adsorption on the conductivity: The conductivity of the reaction mixture was measured in an attempt to assess the leachability of ions during adsorption by the sludges. As illustrated in Fig. 2, for the three sludges studied, the conductivity increased as the reaction time increased. This occurred rapidly within the first 6 h of reaction beyond which there was a gradual change as the system approached equilibrium.

The composition of ions in the supernatant was tested after adsorption. In all instances there was a significant increase sodium ion, released during adsorption, possibly due to ion exchange reactions. Yang *et al*. (2006b) suggested that when alum sludge was added to water, it was surrounded by a tightly bound shell of oriented water molecules (HO-H) on its surface and the positive charge of the alum sludge weakened the forces holding the hydrogen ions (H^+) to the oxygen and were therefore easily released. There was also an observed change in pH which may be accounted for by the release of H^+ and OH^- ions.

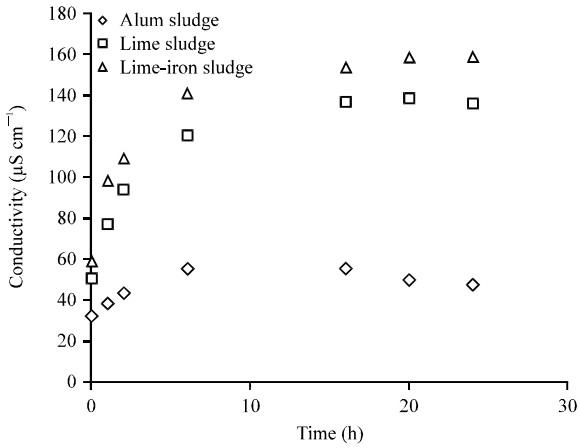

Fig. 2: Leaching of ions resulting from phosphate adsorption by water treatment sludge

CONCLUSION

Batch experiments were conducted to investigate the adsorption kinetics of orthophosphate (potassium dihydrogen phosphate) by water treatment sludge (alum sludge, lime sludge and lime-iron sludge). Experimental parameters were varied and analyzed using four kinetic models in an attempt to expound the adsorption characteristics. Based on the output of the study the following conclusions can be drawn:

- The adsorption potential of water treatment sludge varied with the pH of the reaction solution. Alum sludge favoured slightly acidic suspensions, pH 4 while lime sludge and lime-iron sludge favoured slightly basic conditions (pH 8)
- The entire period of adsorption was successfully simulated using the diffusion-chemisorption model. Generally higher correlation to the linear and non-linear plots was observed over that of the other tested models
- The diffusion-chemisorption model produced an initial rate, overall rate and maximum adsorption capacity which reveal that lime-iron sludge produced the highest capacity of 2.313 mg L^{-1} at pH of 8 and agitation of 250 rpm. This adsorption capacity was 34 and 52% higher than that for lime and alum sludge, respectively
- The time to reach equilibrium was found to be 6 h for all samples tested

ACKNOWLEDGMENT

The authors wish to acknowledge Neal Hassim, Paul Aming, Sarah Mohammed, Rheal Thomas, Donald Mitchell, Vikesh Narrie, Vitra Harry and Garvin Mangal for their valued assistance throughout the research.

REFERENCES

Badmus, M.A.O., T.O.K. Audu and B.U. Anyata, 2007. Removal of lead ion from industrial wastewaters by activated carbon prepared from periwinkle shells (*Typanotonus fuscatus*). Turk. J. Eng. Environ. Sci., 31: 251-263.

Bakyayita, G.K., 2014. Equilibrium and kinetic batch studies of cadmium and lead sorption using low cost biosorbents. Licentiate Thesis, KTH Royal Institute of Technology, Stockholm, Sweden.

Dayton, E.A. and N.T. Basta, 2001. Characterization of drinking water treatment residuals for use as a soil substitute. Water Environ. Res., 73: 52-57.

Duffy, S.J. and G.W. van Loon, 1994. Characterization of amorphous aluminum hydroxide by the ferron method. Environ. Sci. Technol., 28: 1950-1956.

Farrell, P.B., 2012. Global suicide 2020: We can't feed 10 billion. February 14, 2012. http://www.marketwatch.com/story/global-suicide-2020-we-cant-feed-10-billion-2012-02-14

Fernadez, N.A., E. Chacin, E. Gutierrez, N. Alastre, B. Llamoza and C.F. Forster, 1995. Adsorption of lauryl benzyl sulphonate on algae. Bioresour. Technol., 54: 111-115.

Genz, A., A. Kornmuller and M. Jekel, 2004. Advanced phosphorus removal from membrane filtrates by adsorption on activated aluminium oxide and granulated ferric hydroxide. Water Res., 38: 3523-3530.

Gibbons, K.M., M. Mortula and G.A. Gagnon, 2009. Phosphorus adsorption on water treatment residual solids. J. Water Supply: Res. Technol., 58: 1-10.

Hayden, P.L. and A.J. Rubin, 1974. Systematic Investigation of the Hydrolysis and Precipitation of Aluminum (III). In: Aqueous-Environmental Chemistry of Metals, Rubin, A.J. (Ed.). Ann Arbor Science Publishers Inc., Ann Arbor, Michigan, pp: 317-381.

Ho, Y.S. and G. McKay, 1998a. Kinetic model for lead (II) sorption on to peat. Adsorpt. Sci. Technol., 16: 243-255.

Ho, Y.S. and G. McKay, 1998b. Sorption of dye from aqueous solution by peat. Chem. Eng. J., 70: 115-124.

Ho, Y.S., D.A.J. Wase and C.F. Forster, 1996. Kinetic studies of competitive heavy metal adsorption by sphagnum moss peat. Environ. Technol., 17: 71-77.

Ippolito, J.A., F.A. Barbarick, D.N. Heil, J.P. Chandler and E.F. Redente, 2003. Phosphorus retention mechanisms of a water treatment residual. J. Environ. Qual., 32: 1857-1864.

Kim, J.G., J.H. Kim, H.S. Moon, C.M. Chon and J.S. Ahn, 2003. Removal capacity of water plant alum sludge for phosphorus in aqueous solutions. Chem. Speciation Bioavailability, 14: 67-73.

Krim, L., S. Nacer and G. Bilango, 2006. Kinetics of chromium sorption on biomass fungi from aqueous solution. Am. J. Environ. Sci., 2: 27-32.

Kumar, K.V. and S. Sivanesan, 2006. Pseudo second order kinetic models for safranin onto rice husk: Comparison of linear and non-linear regression analysis. Process Biochem., 41: 1198-1202.

Lagergren, S., 1898. About the theory of so-called adsorption of soluble substances. Kungliga Svenska Vetenskapsakademiens Handlingar, 24: 1-39.

Liu, R.X., J.L. Guo and H.X. Tang, 2002. Adsorption of fluoride, phosphate and arsenate ions on a new type of ion exchange fiber. J. Colloid Interface Sci., 248: 268-274.

Mohammed, W.T. and S.A. Rashid, 2012. Phosphorus removal from wastewater using oven-dried alum sludge. Int. J. Chem. Eng., Vol. 2012. 10.1155/2012/125296

Mortula, M.M. and G.A. Gagnon, 2007. Phosphorus treatment of secondary municipal effluent using oven-dried alum residual. J. Environ. Sci. Health, Part A: Toxic/Hazardous Subst. Environ. Eng., 42: 1685-1691.

Namasivayam, C. and K. Ranganathan, 1993. Waste Fe (III)/Cr (III) hydroxide as adsorbent for the removal of Cr (VI) from aqueous solution and chromium plating industry wastewater. Environ. Pollut., 82: 255-261.

Nomanbhay, S.M. and K. Palanisamy, 2005. Removal of heavy metal from industrial wastewater using Chitosan coated oil palm shell charcoal. Electron. J. Biotechnol., 8: 43-53.

Ofomaja, A.E., A. Pholosi and E.B. Naidoo, 2014. Kinetics and competitive modeling of cesium biosorption onto iron (III) hexacyanoferrate modified pine cone powder. Int. Biodeterioration Biodegradation, 92: 71-78.

Panday, K.K., G. Prasad and V.N. Singh, 1985. Copper (II) removal from aqueous solutions by fly ash. Water Res., 19: 869-873.

Rahman, M.A., M.T. Islam, M. Nurnabi and P. Bala, 2013. Kinetics and equilibrium studies of sorption of Remazol G Yellow RGB (An anionic reactive dye) onto acid activated vegetable kitchen waste. Int. J. Environ. Pollut. Control Manage., 5: 72-84.

Razali, M., Y.Q. Zhao and M. Bruen, 2007. Effectiveness of a drinking-water treatment sludge in removing different phosphorus species from aqueous solution. Sep. Purif. Technol., 55: 300-306.

Sharma, D.C. and C.F. Forster, 1996. Removal of hexavalent chromium from aqueous solutions by granular activated carbon. Water SA., 22: 153-160.

Sharma, Y.C., G. Prasad and D.C. Rupainwar, 1991. Removal of Ni (II) from aqueous solutions by sorption. Int. J. Environ. Stud., 37: 183-191.

Sutherland, C. and C. Venkobachar, 2010. A diffusion-chemisorption kinetic model for simulating biosorption using forest macro-fungus, *Fomes fasciatus*. Int. J. Plant Anim. Sci., 1: 107-117.

Sutherland, C., 2004. Removal of heavy metals from waters using low cost adsorbents: Process development. Ph.D. Thesis, University of the West Indies, Trinidad.

Tie, J., D. Chen, X. Li, X. Zhu, Y. Liu and Y. Liu, 2010. Phosphorus adsorption characteristics of alum and iron sludge from drinking-water treatment works. Proceedings of the 4th International Conference on Bioinformatics and Biomedical Engineering, June 18-20, 2010, Chengdu, pp: 1-3.

Weber, W.J. and J.C. Morris, 1962. Advances in water pollution research: Removal of biologicallyresistant pol lutants from waste waters by adsorption. Proceedings of International Conference on Water Pollution Symposium, (ICWPS`62), Pergamon, Oxford, pp: 231-266.

Yang, Y., D. Tomlinson, S. Kennedy and Y.Q. Zhao, 2006a. Dewatered alum sludge: A potential adsorbent for phosphorus removal. Water Sci. Technol., 54: 207-213.

Yang, Y., Y.Q. Zhao, A.O. Babatunde, L. Wang, Y.X. Ren and Y. Han, 2006b. Characteristics and mechanisms of phosphate adsorption on dewatered alum sludge. Sep. Purif. Technol., 51: 193-200.